Environmental Science & Technology

Article

Cite This: Environ. Sci. Technol. 2018, 52, 1496−1505

pubs.acs.org/est

Controlling Ethanol Use in Chain Elongation by CO_2 Loading Rate

Mark Roghair,[†] Tim Hoogstad,[†,#] David P.B.T.B. Strik,[*,†] Caroline M. Plugge,[‡,§] Peer H.A. Timmers,[‡,§] Ruud A. Weusthuis,[∥] Marieke E. Bruins,[⊥] and Cees J. N. Buisman[†]

[†]Sub-department of Environmental Technology, Wageningen University & Research, Bornse Weilanden 9, 6708 WG, Wageningen, The Netherlands

[‡]Laboratory of Microbiology, Wageningen University & Research, Stippeneng 4, 6708 WE, Wageningen, The Netherlands

[§]Wetsus, European Centre of Excellence for Sustainable Water Technology, Oostergoweg 9, 8911 MA Leeuwarden, The Netherlands

[∥]Bioprocess Engineering, Wageningen University & Research, Droevendaalsesteeg 1, 6708 PB, Wageningen, The Netherlands

[⊥]Wageningen Food & Biobased Research, Wageningen University & Research, Bornse Weilanden 9, 6708 WG, Wageningen, The Netherlands

Supporting Information

ABSTRACT: Chain elongation is an open-culture biotechnological process which converts volatile fatty acids (VFAs) into medium chain fatty acids (MCFAs) using ethanol and other reduced substrates. The objective of this study was to investigate the quantitative effect of CO_2 loading rate on ethanol usages in a chain elongation process. We supplied different rates of CO_2 to a continuously stirred anaerobic reactor, fed with ethanol and propionate. Ethanol was used to upgrade ethanol itself into caproate and to upgrade the supplied VFA (propionate) into heptanoate. A high CO_2 loading rate (2.5 $L_{CO2}{\cdot}L^{-1}{\cdot}d^{-1}$) stimulated excessive ethanol oxidation (EEO; up to 29%) which resulted in a high caproate production (10.8 $g{\cdot}L^{-1}{\cdot}d^{-1}$). A low CO_2 loading rate (0.5 $L_{CO2}{\cdot}L^{-1}{\cdot}d^{-1}$) reduced EEO (16%) and caproate production (2.9 $g{\cdot}L^{-1}{\cdot}d^{-1}$). Heptanoate production by VFA upgrading remained constant (~1.8 $g{\cdot}L^{-1}{\cdot}d^{-1}$) at CO_2 loading rates higher than or equal to 1 $L_{CO2}{\cdot}L^{-1}{\cdot}d^{-1}$. CO_2 was likely essential for growth of chain elongating microorganisms while it also stimulated syntrophic ethanol oxidation. A high CO_2 loading rate must be selected to upgrade ethanol (e.g., from lignocellulosic bioethanol) into MCFAs whereas lower CO_2 loading rates must be selected to upgrade VFAs (e.g., from acidified organic residues) into MCFAs while minimizing use of costly ethanol.

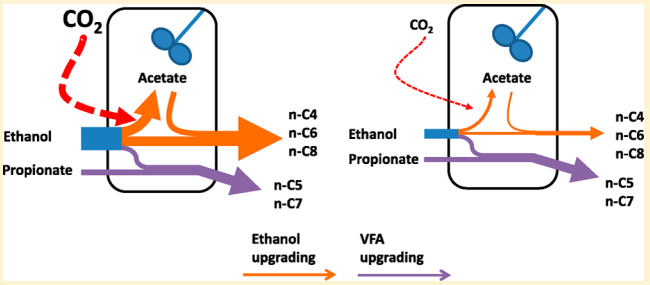

1. INTRODUCTION

Medium chain fatty acids (MCFAs) are straight-chain monocarboxylic acids with 6 to 10 carbon atoms. These molecules can serve as precursors for production of fuels and other chemicals.[1] Conventional methods to produce MCFAs use vegetable oils (palm kernel oil, coconut oil, and castor oil) from oil seed crops.[2,3] Growing these crops for production of fuels and chemicals, however, competes with human food production (i.e., arable land) and is associated with loss of water resources and biodiversity.[4,5] Organic residues from agriculture or food industry are interesting alternative feedstocks for the production of MCFAs because they are renewable, abundantly available and their application does not compete with human food production. In addition, these residues must often be treated to prevent environmental pollution. An emerging open-culture biotechnological process that facilitates valorization of organic residues into MCFAs is chain elongation. Chain elongation is a secondary fermentation process within the carboxylate platform.[1] It is known to ferment volatile fatty acids (VFAs; acetate, propionate and butyrate) as electron acceptor together with ethanol as electron donor into MCFAs through the reverse β-oxidation pathway. In this pathway, 1 mol of ethanol is anaerobically oxidized into acetate for every 5 chain elongation reactions, yielding one ATP via substrate level phosphorylation (eq 1 and Supporting Information (SI) Table S1).

$$\text{reverse } \beta-\text{oxidation pathway } 5C_xH_{2x-1}O_2^- + 6C_2H_6O \rightarrow 5C_{x+2}H_{2x+3}O_2^- + C_2H_3O_2^- + 4H_2O + H^+ + 2H_2 \quad (1)$$

Chain elongation has been demonstrated with synthetic medium,[6−9] with organic residues such as acidified garden- and kitchen waste,[10] acidified organic fraction of municipal solid waste[11] and with undistilled fermentation broth from the bioethanol industry.[12,13]

VFAs for chain elongation can be obtained by hydrolysis and acidification (primary fermentation) of organic residues,

Received: September 21, 2017
Revised: December 1, 2017
Accepted: January 5, 2018
Published: January 5, 2018

DOI: 10.1021/acs.est.7b04904
Environ. Sci. Technol. 2018, 52, 1496−1505

making them inexpensive substrates. Although electron donors such as methanol[14] or lactate[15] have been successfully used, ethanol is the preferred electron donor for high-rate chain elongation.[16] Ethanol can be introduced in three ways: (1) it can be present within the feedstock itself, (2) it can be produced in situ from the feedstock (e.g., by fermentation of sugars) or (3) it can be procured off site and added to the chain elongation reactor.[16] Ethanol, however, is a costly substrate. Knowledge on the mechanisms of the use of ethanol is therefore essential to establish an ethanol-efficient chain elongation process.

In a chain elongation process, ethanol is primarily used by chain elongating microorganisms (e.g., *Clostridium kluyveri*[6,17]) through the reverse β-oxidation pathway. Since we use an open culture process, however, typically several competing biochemical processes occur as a result of consumption of supplied substrates or produced intermediates. For example, increased ethanol oxidation to acetate at a ratio different from the 5:1 ratio has also been observed in chain elongation cultures.[11] This is caused by direct oxidation of ethanol and is also known as excessive ethanol oxidation (EEO; eq 2 and SI Table S1). EEO is considered to be performed by ethanol-oxidizing microorganisms which do not perform chain elongation, but these microorganisms have not been identified yet. Although it could be possible that EEO is performed by chain elongating microorganisms through a more flexible 5:1 ratio in the reverse β-oxidation pathway, we assume in this study that this ratio does not change and that EEO is performed through direct oxidation of ethanol. Another process that proceeds in chain elongation cultures is hydrogenotrophic methanogenesis (eq 3 and SI Table S1). This process does not consume VFAs, ethanol or MCFAs directly[11,12] but it consumes a part of the produced components within the open culture.

$$\text{excessive ethanol oxidation (EEO)} \quad C_2H_6O + H_2O \rightarrow C_2H_3O_2^- + H^+ + 2H_2 \tag{2}$$

$$\text{hydrogenotrophic methanogenesis} \quad 4H_2 + CO_2 \rightarrow CH_4 + 2H_2O \tag{3}$$

Ethanol use in chain elongation is not straightforward because ethanol is not only used to elongate (i.e., upgrade) VFAs into MCFAs but also because it can be used to upgrade ethanol itself into MCFAs. To identify the different uses of ethanol, we distinguish two types of carbon fluxes which lead to the production of MCFAs: VFA upgrading (eq 2a and b, SI Table S1) and ethanol upgrading (eq 1a–e, SI Table S1). VFA upgrading is chain elongation of VFAs (through the reverse β-oxidation pathway) which are derived from primary fermentation and which are **not** derived from in situ ethanol oxidation into acetate. Ethanol upgrading is a combination of (1) in situ ethanol oxidation into acetate (through both EEO and the reverse β-oxidation pathway) and (2) subsequent chain elongation of this in situ produced acetate into even-numbered fatty acids (through the reverse β-oxidation pathway). Both VFA upgrading and ethanol upgrading are not self-contained biochemical processes or pathways. Rather, whereas VFA upgrading is a result from only a part of the reverse β-oxidation pathway, ethanol upgrading is a result from a combination of in situ ethanol oxidation and the reverse β-oxidation pathway. Because EEO, ethanol upgrading and VFA upgrading are simultaneous and intertwined fluxes, previous studies could not quantify via which route MCFAs were produced (e.g., refs 11 and 8). As such, it was not determined how much ethanol was effectively used for MCFA production.

CO_2 affects both chain elongating microorganisms and ethanol oxidizers. The well described chain elongating bacterium *C. kluyveri* requires CO_2 for anabolic reactions.[18] CO_2 has also been shown to influence EEO. When the CO_2 concentration is sufficiently low, hydrogenotrophic methanogenic activity is suppressed, and the resulting higher hydrogen concentration inhibits EEO.[11,13] Because CO_2 influences EEO and because the resulting acetate could stimulate the carbon flux of ethanol upgrading, CO_2 loading rate may be an important control parameter in the conversion of an ethanol-rich feedstock into MCFAs through ethanol upgrading. To date, there are no studies that describe the effect of CO_2 on chain elongation while specifically distinguishing ethanol upgrading and VFA upgrading. In addition, the concurring archaeal community involved in methane formation has not been characterized.

The objective of this study was to investigate the quantitative effect of CO_2 loading rate on ethanol use in a chain elongation process. Ethanol upgrading and VFA upgrading were studied by supplying different loading rates of gaseous CO_2 to a continuously stirred anaerobic reactor with granular and suspended chain elongation sludge.[19] By using propionate as VFA instead of acetate, a distinction between the carbon flux of ethanol upgrading (represented by even-numbered fatty acids) and the carbon flux of VFA upgrading (represented by odd-numbered fatty acids) was conceived. In addition, the microbial community was analyzed to compare the microbial communities at different CO_2 loading rates.

2. MATERIALS AND METHODS

2.1. Experimental Setup, Procedure, and Analysis. This study used a continuously stirred anaerobic reactor as described by Roghair et al. (2016).[19] In short, a continuous reactor (Volume 1 L) with granular and suspended chain elongation sludge was operated at 30 °C, 1 atm, *p*H 6.8 (by addition of 2 M NaOH), stirred at 100 rpm with a hydraulic retention time (HRT) of 17 h. Gaseous CO_2 was supplied with a mass-flow controller (Brooks Instruments 5850S, The Netherlands). The reactor was continuously fed with a synthetic medium that contained propionate (10.9 $g \cdot L^{-1} \cdot d^{-1}$) and ethanol. During the study, different CO_2 loading rates were applied: 2.5 $L_{CO2} \cdot L^{-1} \cdot d^{-1}$ (day 0–124), 1 $L_{CO2} \cdot L^{-1} \cdot d^{-1}$ (day 124–187), 0.5 $L_{CO2} \cdot L^{-1} \cdot d^{-1}$ (day 187–211), 0 $L_{CO2} \cdot L^{-1} \cdot d^{-1}$ (day 211–224) and again 1 $L_{CO2} \cdot L^{-1} \cdot d^{-1}$ (day 224–240). The first 119 days of the reactor operation has been presented in a previous study.[19] Steady state data of this previous study (2.5 $L_{CO2} \cdot L^{-1} \cdot d^{-1}$) is presented here again to place it in the context of steady state intervals from this study.

Ethanol loading rates were 16.3 $g \cdot L^{-1} \cdot d^{-1}$ (at 1, 0.5, and 0 $L_{CO2} \cdot L^{-1} \cdot d^{-1}$) and 32.5 $g \cdot L^{-1} \cdot d^{-1}$ (at 2.5 $L_{CO2} \cdot L^{-1} \cdot d^{-1}$). The ethanol loading rate at 1.0, 0.5, and 0 $L_{CO2} \cdot L^{-1} \cdot d^{-1}$ was twice as low as compared to the initial CO_2 loading rate (2.5 $L_{CO2} \cdot L^{-1} \cdot d^{-1}$). This was performed to prevent ethanol toxicity because with lower CO_2 loading rates, ethanol consumption rates decreased, resulting in increased ethanol concentrations. Ethanol concentrations during selected steady state intervals were in a range in which chain elongation is known to occur and were between 0.7 ± 0.5 $g \cdot L^{-1}$ (1 $L_{CO2} \cdot L^{-1} \cdot d^{-1}$) and 8.7 ± 0.7 $g \cdot L^{-1}$ (no CO_2 loading rate). The reactor was in steady state when net production and consumption rates of fatty acids and ethanol were similar (maximum relative standard deviation of

DOI: 10.1021/acs.est.7b04904
Environ. Sci. Technol. 2018, 52, 1496–1505

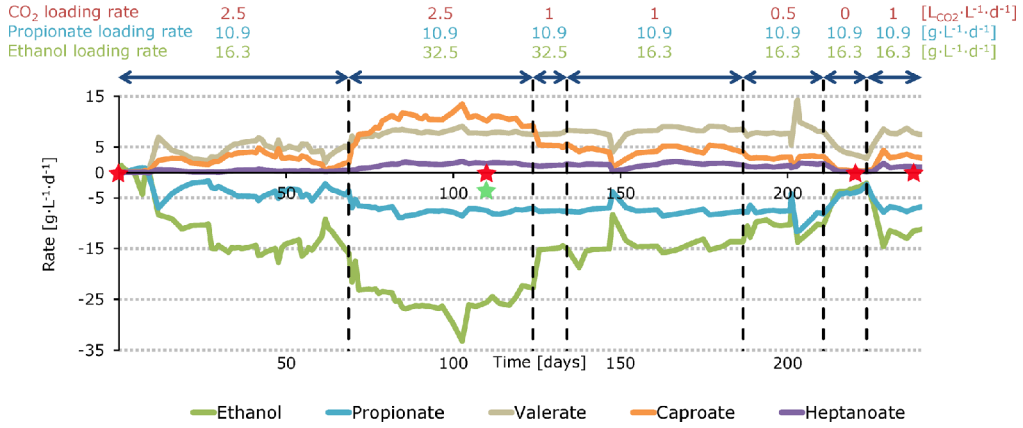

Figure 1. Graphical summary of the effect of CO_2 loading rate on reactor performance with net production and consumption rates over time. At the red stars, samples for bacterial community analysis were taken. At the green star, a sample for archaeal community analysis was taken. T = 30 °C, pH 6.8, HRT = 17 h, V = 1 L.

20%) over a period of at least 5 days (7 HRTs). Caprylate was excluded from this criterion because this compound was produced in insignificant amounts. Results that we present and discuss are based on steady states unless mentioned otherwise. Standard deviations are based on at least four measurements.

Analytical procedures for fatty acids (C2−C8), alcohols (C2−C3) and for determination of the headspace composition (CO_2 and CH_4) were the same as described previously.[19] Propanol was measured on the same column as ethanol although this was not formerly mentioned. In addition, hydrogen in the headspace was determined by GC.[20] Liquid samples were taken from the reactor content 3−5 times per week whereas gas samples from the headspace were taken once per week.

Samples for microbial community analysis were taken on day 1, 2, and 3 (pooled together; initial bacterial community), day 110 (2.5 $L_{CO2}·L^{-1}·d^{-1}$), day 219, 222, and 224 (pooled together; 0 $L_{CO2}·L^{-1}·d^{-1}$) and on day 238 (1 $L_{CO2}·L^{-1}·d^{-1}$). These samples were divided into granular and suspended sludge fractions by allowing granules to settle. After separation, suspended sludge fractions eventually did not contain visible granules and granular sludge fractions were washed three times with 1× phosphate-buffered saline to remove residual suspended sludge. Bacterial community analysis was performed on all samples using high-throughput 16S rRNA gene sequencing. Archaeal community analysis was performed on one sample, suspended sludge at 2.5 $L_{CO2}·L^{-1}·d^{-1}$, by using 16S rRNA gene cloning. This sample was selected based on the highest methane production rate in the operational period. Details on the materials and methods for microbial community analysis (DNA extraction, bacterial community analysis and archaeal community analysis) are reported in the Supporting Information (SI).

2.2. Calculations on Carbon Fluxes for Carbon Flux Analysis. Calculations on carbon fluxes are shown in SI Table S2. These calculations are based on net production and consumption rates (under steady state conditions) and on the stoichiometric equations in SI Table S1. Total ethanol use was divided into (1) excessive ethanol oxidation, (2) ethanol oxidation through the reverse β-oxidation pathway, and (3) ethanol use for elongation of fatty acids through the reverse β-oxidation pathway. Total CO_2 use was divided into (1) CO_2 use by hydrogenotrophic methanogenesis and (2) unidentified CO_2 use (i.e., biomass).

Carbon selectivity is based on product formed divided by total substrates consumed.

2.3. Calculations on Change in Gibbs Free Energy for Thermodynamic Analysis. Thermodynamic calculations were performed as described by Kleerebezem et al. (2010) using their provided ΔG_f^0 and ΔH_f^0 values for individual components.[21] Temperature corrections to 30 °C were made using the Gibbs−Helmholtz equation. Thermodynamic limits for hydrogen partial pressures (pH_2) of EEO and the reverse β-oxidation pathway were determined in the same way as was performed by Ge et al. (2015).[22]

3. RESULTS

3.1. Bioreactor Performance at Different CO_2 Loading Rates. CO_2 loading rate was shown to be an effective control parameter in chain elongation. CO_2 was essential for caproate, heptanoate and caprylate (MCFA) production and it especially stimulated ethanol upgrading to caproate. Caprylate production was insignificant and hence the effect of CO_2 on caprylate production was not shown in this study. A graphical summary of the effect of CO_2 loading rate on reactor performance can be seen in Figure 1 (rate in $g·L^{-1}·d^{-1}$) and SI Figure S1 (rate in mmol $C·L^{-1}·d^{-1}$). Mean steady state values of reactor concentrations, rates and carbon selectivity values can be seen in SI Table S3−S7.

The reactor was started with a high CO_2 loading rate (2.5 $L_{CO2}·L^{-1}·d^{-1}$). Through the first stage, the reactor did not reach a steady state. Yet, it was noticed that ethanol became depleted which likely limited MCFA production rates. The ethanol loading rate, therefore, was increased on day 68 from 16.3 to 32.5 $g·L^{-1}·d^{-1}$. Thereafter, a steady state of 27 days was observed as was presented previously.[19] Here, caproate was produced at 10.8 ± 0.5 $g·L^{-1}·d^{-1}$ at a concentration of 7.4 ± 0.2 $g·L^{-1}$ while heptanoate was produced at 1.8 ± 0.1 $g·L^{-1}·d^{-1}$ at a concentration of 1.2 ± 0.1 $g·L^{-1}$. Caproate must have been produced by ethanol upgrading because other even-numbered fatty acids (acetate or butyrate) were not fed to the reactor. Heptanoate must have been produced by VFA upgrading starting with propionate because (1) propionate was the only VFA that was fed to the reactor and (2) chain elongation of propionate results in production of heptanoate.[9]

On day 124, we decreased the CO_2 loading rate from 2.5 to 1 $L_{CO2}·L^{-1}·d^{-1}$ after which a steady state of 8 days was observed (steady state characteristics are not shown). Here, caproate was

DOI: 10.1021/acs.est.7b04904
Environ. Sci. Technol. 2018, 52, 1496−1505

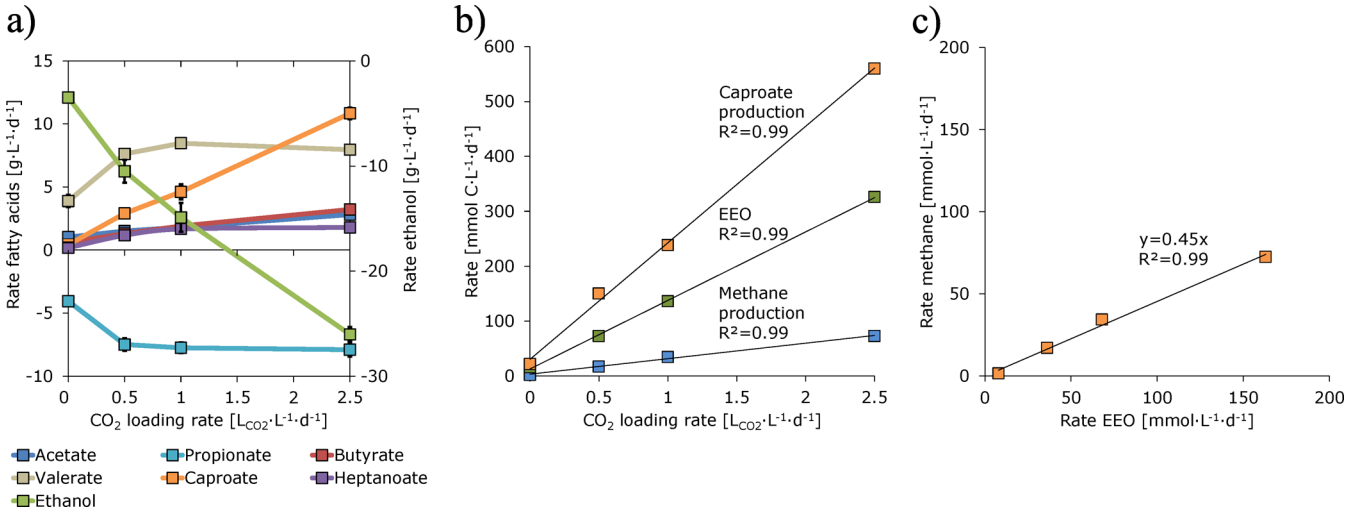

Figure 2. (a) Net production and consumption rates of fatty acids and ethanol at different CO_2 loading rates (bars indicate standard deviations but are often too small to be visual), (b) carbon flux of EEO, caproate production and methane production at different CO_2 loading rates, (c) rate of methane vs EEO. Presented values at 0 $L_{CO2}·L^{-1}·d^{-1}$ are not steady state values but averages. Regression line = —.

produced at a ~ two times lower rate (5.3 ± 0.3 $g·L^{-1}·d^{-1}$) while heptanoate was produced at a slightly lower rate (1.4 ± 0.2 $g·L^{-1}·d^{-1}$) compared to the steady state at 2.5 $L_{CO2}·L^{-1}·d^{-1}$. Because ethanol was consumed at a lower rate, its concentration increased from 3.7 ± 1.4 $g·L^{-1}$ to 11.6 ± 0.8 $g·L^{-1}$. To prevent potential ethanol toxicity (e.g., ref 23), we decreased the ethanol loading rate from 32.5 to 16.3 $g·L^{-1}·d^{-1}$ on day 134. Thereafter, a steady state was observed of 40 d in which caproate (4.6 ± 0.6 $g·L^{-1}·d^{-1}$) and heptanoate (1.7 ± 0.3 $g·L^{-1}·d^{-1}$) were produced at similar rates as before the decrease in ethanol loading rate. This shows that a change in ethanol loading rate and concentration does not substantially influence reactor performance as long as ethanol is not depleted.

On day 187, the CO_2 loading rate was further decreased from 1 to 0.5 $L_{CO2}·L^{-1}·d^{-1}$ after which we observed another steady state of 13 days. Here, caproate was produced at a 73% lower rate (2.9 ± 0.2 $g·L^{-1}·d^{-1}$) while heptanoate was produced at a 35% lower rate (1.2 ± 0.2 $g·L^{-1}·d^{-1}$) compared to the steady state at 2.5 $L_{CO2}·L^{-1}·d^{-1}$. On day 211, we cut off the CO_2 supply (0 $L_{CO2}·L^{-1}·d^{-1}$). From then on, the microbiome failed in effective chain elongation as we noticed low and decreasing MCFA production rates (<0.5 $g·L^{-1}·d^{-1}$). Because rates kept on decreasing the reactor did not reach a steady state. To prevent a total collapse, the CO_2 loading rate was increased from 0 to 1 $L_{CO2}·L^{-1}·d^{-1}$ on day 224. This resulted in a revival of the microbiome as we observed, later on, similar steady state rates as before with the same CO_2 loading rate. A summary on net production and consumption rates of fatty acids and ethanol at different CO_2 loading rates in shown in Figure 2a. An overview and characteristics of the steady states is shown in Table 1.

3.2. Excessive Ethanol Oxidation and the Fate of Propionate. The highest rate of EEO was observed when the CO_2 loading rate was 2.5 $L_{CO2}·L^{-1}·d^{-1}$ (7.5 $g·L^{-1}·d^{-1}$; Table 1). EEO (1.7 $g·L^{-1}·d^{-1}$) could be reduced with 77% when the CO_2 loading rate was decreased to 0.5 $L_{CO2}·L^{-1}·d^{-1}$ but was still observed when CO_2 was not supplied. A part of the acetate produced by EEO was used as electron acceptor for ethanol upgrading. In the period with the highest rate of ethanol upgrading (2.5 $L_{CO2}·L^{-1}·d^{-1}$), this acetate consumption for ethanol upgrading was 7.9 $g·L^{-1}·d^{-1}$. Because the reverse β-oxidation pathway could maximally produce 4 $g·L^{-1}·d^{-1}$ (51%), the remaining 49% acetate that served as electron acceptor for ethanol upgrading must have been produced by EEO. Ethanol upgrading was therefore found to be clearly mediated by EEO.

Propanol production (0.5−1.2 $g·L^{-1}·d^{-1}$) was observed throughout the entire study and was likely formed by reduction of propionate with hydrogen. Propanol can still be used as electron donor for chain elongation of acetate if not for propionate elongation. Because all consumed propionate was used for propanol production and chain elongation to heptanoate and valerate (with a carbon closure of 95−102%) it is unlikely that propanol served as electron donor for MCFA production or that propionate was oxidized into acetate. As such, the carbon flux of ethanol upgrading and VFA upgrading were not complicated by propanol elongation or propionate oxidation.

3.3. Microbial Community: Abundance of Clostridiales and *Methanobrevibacter acididurans*. The bacterial community was analyzed using high throughput 16S rRNA amplicon sequencing to identify changes at different CO_2 loading rates in the chain elongation process. This was performed for both the granular and suspended sludge fraction. The *Clostridiales* order consistently dominated the bacterial community irrespective of CO_2 loading rate or sludge type (Figure 3 and SI Figure S3). *Clostridiales* had the highest relative abundance in all reactor samples (53−77%), followed by *Bacteroidales* (3−18%) and *Erysipelotrichales* (1−12%). Most *Clostridiales* were identified as members of the *Clostridiaceae* family. Dominance of *Clostridiaceae*, with *C. kluyveri* as well-known member and model species for chain elongation, has been frequently observed.[17,6]

Minor changes in the bacterial community were observed during the operational period which do not seem to link with the CO_2 loading rate. An increase in relative abundance (compared to the initial bacterial community) was observed for several operational taxonomic units. *Erysipelotrichales* and *Selenomonadales* increased in relative abundance as compared to the initial bacterial community, especially in the granular sludge fraction. *Desulfovibrionales* increased in relative abundance as compared to the initial bacterial community in both granular and suspended sludge fractions.

DOI: 10.1021/acs.est.7b04904
Environ. Sci. Technol. 2018, 52, 1496−1505

Table 1. Overview and Characteristics of Steady States. Concentrations, Rates and Carbon Selectivities Are Reported in SI Tables S3–S7

CO_2 loading rate	propionate/ethanol loading rate	steady state interval	mean product formation rate				mean EEO	mean headspace gas composition			CO_2 in liquid[a]
[$L_{CO2}·L^{-1}·d^{-1}$]	[$g·L^{-1}·d^{-1}$]	[d]	caproate [$g·L^{-1}·d^{-1}$]	heptanoate [$g·L^{-1}·d^{-1}$]	CH_4 [$mmol·L^{-1}·d^{-1}$]	[$g·L^{-1}·d^{-1}$] (% of total ethanol use)	pCH_4 [%]	pH_2 [%]	pCO_2 [%]	[$mmol·L^{-1}$]
high [2.5]	10.9/32.5	84–97, 105–119	10.8	1.8	72.6	7.5 (28.8%)	91.9	0.03	4.6	1.42
medium [1.0]	10.9/16.3	155–187	4.6	1.7	34.3	3.1 (21.0%)	92.2	0.08	2.3	0.71
low [0.5]	10.9/16.3	188–201	2.9	1.2	17.1	1.7 (15.9%)	87.9	0.20	1.1	0.34
none [0.0]	10.9/16.3	NA[b]	0.4	0.2	1.5	0.4 (10.5%)	49.3	41.6	0.07	0.03
medium [1.0]	10.9/16.3	229–240	3.3	1.2	29.6	2.5 (20.7%)	93.1	0.08	1.4	0.44

[a]Calculated from the gaseous CO_2 concentration in the headspace by Henry's law at 1 atm and 30 °C.[24] [b]Not applicable because there was no steady state observed. Presented values at 0 $L_{CO2}·L^{-1}·d^{-1}$ are averages.

CO_2 loading rate [$L_{CO2}·L^{-1}·d^{-1}$] →	High [2.5]		Medium [1.0]		None [0.0]	
Order ↓	IBC	Granular	Suspended	Granular	Suspended	Granular	Suspended
Bacteroidales	20	11	10	3	18	8	8
Bacillales	3	0	0	0	1	0	0
Lactobacillales	11	1	7	1	9	2	5
Clostridiales	62	71	71	75	53	64	77
Erysipelotrichales	0	12	7	8	4	12	1
Selenomonadales	0	2	1	10	4	11	5
Burkholderiales	1	0	1	0	6	0	1
Desulfovibrionales	1	3	2	3	4	2	2
Other	1	0	0	1	2	1	1

Figure 3. Heatmap of bacterial community at different CO_2 loading rates in granular and suspended sludge. Numbers indicate percentage relative abundance. "Other" are specified in Figure S3. The ethanol loading rate at 2.5 $L_{CO2}·L^{-1}·d^{-1}$ was 32.2 $g·L^{-1}·d^{-1}$ whereas the ethanol loading rate at 1.0 and 0.0 $L_{CO2}·L^{-1}·d^{-1}$ was 16.3 $g·L^{-1}·d^{-1}$. IBC = initial bacterial community.

The archaeal community in suspended sludge at 2.5 $L_{CO2}·L^{-1}·d^{-1}$ was analyzed by 16S rRNA gene cloning and Sanger sequencing. 95 out of 96 clones showed highest identity with *Methanobrevibacter acididurans* (97–99% sequence identity; SI Table S8). This means that we have specifically identified a hydrogenotrophic methanogen in a chain elongation process whereas no acetotrophic methanogens were detected.

4.0. DISCUSSION

4.1. Ethanol Upgrading: CO_2 Stimulates Excessive Ethanol Oxidation and Caproate Production. In our study, we identified three dominant biochemical processes that converted the supplied substrates and/or produced intermediates: (1) chain elongation (through the reverse β-oxidation pathway; eq 1),[25] (2) excessive ethanol oxidation (EEO; eq 2),[11] and (3) hydrogenotrophic methanogenesis (eq 3).[11,12] They were identified based on processes that are known to occur in chain elongation reactors and on a stoichiometric carbon flux analysis of our results. Acetotrophic methanogenesis was not identified in this carbon flux analysis. This was confirmed by our archaeal community analysis in which no acetotrophic methanogens were detected. We consider that each process is performed by a corresponding functional group of microorganisms; chain elongation is performed by chain elongating microorganisms, EEO is performed by ethanol oxidizers and methanogenesis by hydrogenotrophic methanogens.

A Sankey diagram was made to illustrate the role of the three functional groups in the carbon fluxes at high (2.5 $L_{CO2}·L^{-1}·d^{-1}$) and at low (0.5 $L_{CO2}·L^{-1}·d^{-1}$) CO_2 loading rate (Figure 4). Although ethanol loading rates were also different at these selected CO_2 loading rates, the resulting mean ethanol concentrations were similar (81.3 $mmol·L^{-1}$ at 2.5 $L_{CO2}·L^{-1}·d^{-1}$ and 70.1 $mmol·L^{-1}$ at 0.5 $L_{CO2}·L^{-1}·d^{-1}$), which makes these conditions comparable. Ethanol upgrading (orange arrows) was mediated by ethanol oxidizers and chain elongating microorganism because both EEO and chain elongation (of even-numbered fatty acids) attributed to this carbon flux. VFA upgrading (purple arrows) was mediated by chain elongating microorganisms because only chain elongation (of odd-numbered fatty acids) attributed to this carbon flux. Methane production was performed by hydrogenotrophic methanogens which presumably operated in syntrophy with ethanol oxidizers (see also explanation on the microbial analysis below).

The determined carbon flux analysis provided a linear effect of CO_2 loading rate on caproate production, EEO and on methane production (Figure 2a and b). This shows that these processes were collectively controlled by the CO_2 loading rate

DOI: 10.1021/acs.est.7b04904
Environ. Sci. Technol. 2018, 52, 1496–1505

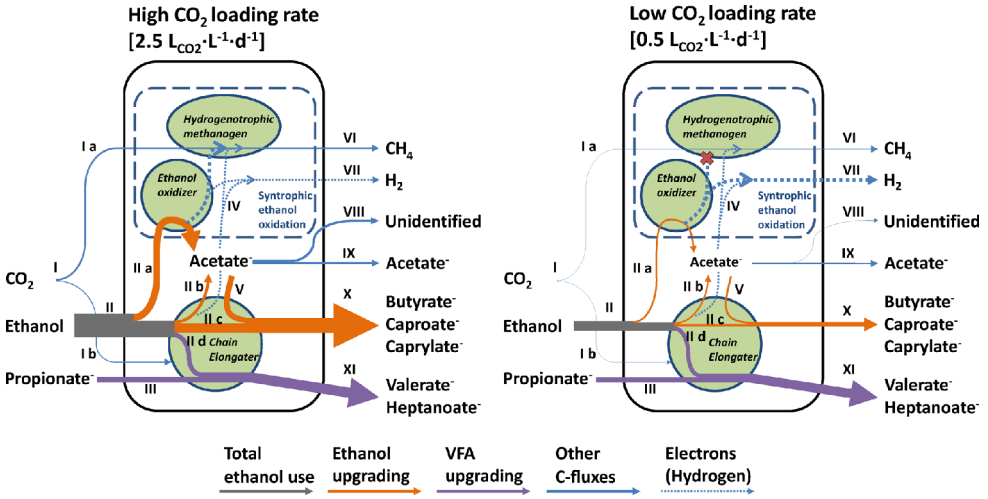

Figure 4. Sankey diagram with observed and calculated carbon fluxes at high (2.5 $L_{CO2}·L^{-1}·d^{-1}$) and low (0.5 $L_{CO2}·L^{-1}·d^{-1}$) CO_2 loading rate. Widths of arrows are proportional to carbon fluxes. Three functional groups of microorganisms (hydrogenotrophic methanogens, ethanol oxidizers, and chain elongating microorganisms) are indicated as green shapes. Calculations on carbon fluxes and numerical values are shown in SI Table S2. (I) Total CO_2 use, (I a) CO_2 use by methanogens, (I b) unidentified CO_2 use (i.e., biomass), (II) total ethanol use, (II a) excessive ethanol oxidation (EEO), (II b) ethanol oxidation through the reverse β-oxidation pathway, (II c) ethanol use for elongation of fatty acids through the reverse β-oxidation pathway (even), (II d) ethanol use for elongation of fatty acids through the reverse β-oxidation pathway (odd), (III) propionate use for VFA upgrading, (IV) (interspecies) hydrogen transfer, (V) acetate use for ethanol upgrading, (VI) methane production, (VII) hydrogen production, (VIII) unidentified acetate use (i.e., biomass), (IX) acetate production, (X) butyrate, caproate and caprylate production by ethanol upgrading, (XI) valerate and heptanoate production by VFA upgrading.

in the tested range. This can be explained as follows: CO_2 was the limiting substrate for hydrogenotrophic methanogenic activity because higher CO_2 loading rates resulted in higher rates of CO_2 consumption and higher rates of methane production (SI Table S3–S6). A high CO_2 loading rate, therefore, stimulated hydrogenotrophic methanogens which, in turn, provided favorable conditions for ethanol oxidizers by lowering the hydrogen partial pressure (pH_2). This explanation is in line with our results because a lower CO_2 loading rate did lead to a higher pH_2 (Table 1). Because of the lower pH_2 at a high CO_2 loading rate, more ethanol was oxidized by EEO and thus more acetate was available as electron acceptor for chain elongation into even-numbered fatty acids (i.e., ethanol upgrading). The concentration of acetate was thus limiting caproate production. Vice versa, a low CO_2 loading rate limited hydrogenotrophic methanogenic activity which resulted in an increased pH_2. This increased pH_2 made EEO thermodynamically less favorable and this resulted into less available acetate for caproate production. Next to acetate, chain elongating microorganisms were possibly also directly limited by CO_2 (Section 4.3). Although the effect of CO_2 on EEO has been shown previously,[11,13] this study demonstrates the effect of CO_2 on ethanol upgrading in a chain elongation process.

The thermodynamic analysis provided the change in Gibbs free energy of various processes at different CO_2 loading rates under actual bioreactor conditions (SI Figure S2). This analysis gives further insights on the determined carbon fluxes. EEO was thermodynamically feasible at 0.5, 1, and 2.5 $L_{CO2}·L^{-1}·d^{-1}$ ($\Delta Gr' < -20$ kJ·reaction^{-1}) but was thermodynamically inhibited at 0 $L_{CO2}·L^{-1}·d^{-1}$ ($\Delta Gr' > -20$ kJ·reaction^{-1}). This was due to the pH_2, which was at least 200 times lower when CO_2 was supplied (0.5, 1, and 2.5 $L_{CO2}·L^{-1}·d^{-1}$) compared to when CO_2 was not supplied (0 $L_{CO2}·L^{-1}·d^{-1}$; Table 1). EEO (0.4 $g·L^{-1}·d^{-1}$), however, was still observed at 0 $L_{CO2}·L^{-1}·d^{-1}$. This reaction could have been enabled at aberrant local conditions (i.e., lower pH_2); for example, inside a granule by hydrogenotrophic methanogens.[26] This process could also have been executed by chain elongating micro-organisms through a more flexible reverse β-oxidation pathway. However, as mentioned before, we assume that the reverse β-oxidation pathway is not flexible and that EEO is executed by ethanol oxidizers which do not perform chain elongation. The reverse β-oxidation pathway (ethanol oxidation coupled to 5× propionate elongation) was thermodynamically feasible at all applied CO_2 loading rates ($\Delta Gr' < -20$ kJ·reaction^{-1}). Other reverse β-oxidation reactions (ethanol oxidation coupled to 5 x acetate, butyrate or valerate elongation) were also feasible since their thermodynamic values were in the same order of magnitude (data not shown). We calculated that the reverse β-oxidation pathway is still feasible even when the pH_2 is extremely high (1000 bar). This shows that the reverse β-oxidation pathway is thermodynamically not hindered by the CO_2 loading rate and by its corresponding pH_2.

We also used the thermodynamic analysis to confirm whether the in situ produced acetate was a result of ethanol oxidation and not from other processes such as propionate oxidation (eq 5, SI Table S1) or homoacetogenesis (eq 6, SI Table S1). Our calculations show that both of these processes were thermodynamically inhibited when CO_2 was supplied ($\Delta Gr' > -20$ kJ·reaction^{-1}). True, these processes could still have occurred at aberrant local conditions. However, even if they occurred, it would have been at negligibly low rates. Propionate oxidation could be neglected because, as mentioned before, propionate was primarily used for production of propanol, valerate, and heptanoate. Also based on stoichiometrics, homoacetogenesis could be neglected because the unidentified CO_2 use (that could have contributed to homoacetogenesis) was at most 33 mmol $C·L^{-1}·d^{-1}$; only ~2% of the total carbon flux. Even this value, though, is overestimated because a part of the unidentified CO_2 use was likely used for growth of chain elongating microorganisms (Section 4.3).

DOI: 10.1021/acs.est.7b04904
Environ. Sci. Technol. 2018, 52, 1496–1505

Grootscholten et al. (2013) also reported increased caproate production rates in a chain elongation process after increasing the CO_2 concentration by doubling the amount of K_2CO_3 in the influent from 4 to 8 g·L^{-1}.[8] Although they did not attribute this observation specifically to ethanol upgrading, increased caproate production was likely a result of this carbon flux. However, because acetate was also present in their influent medium, increased caproate production could (partly) also have been the result of chain elongation of fed acetate (i.e., VFA upgrading). In a later stage of their fermentation study they applied gaseous CO_2 (4.8 L_{CO2}·L^{-1}·d^{-1}), but that did not result in improved caproate production rates, implying that ethanol upgrading was not limited by CO_2 anymore. Eventually, they concluded that their system was limited by (one of the components in) yeast extract. This shows that high-rate ethanol upgrading only proceeds when sufficient growth factors and nutrients are available.

Both EEO and hydrogenotrophic methanogenesis increased with increasing CO_2 loading rate (Figure 2b). The rates of these processes are plotted against each other in Figure 2c. The slope of the plot shows that for every mole of ethanol oxidized by EEO, 0.45 mol of methane is produced. This value is close to the stoichiometric ratio of 0.5 mol methane produced per mole ethanol oxidized in syntrophic ethanol oxidation (SI Table S1), indicating that EEO is a result of the identified syntrophic process.

Electrons (in the form of hydrogen) that did not end up as methane were likely used to reduce propionate into propanol (up to 20 mmol·L^{-1}·d^{-1}) or left the reactor as hydrogen in exhaust gas (up to 1.1 mmol·L^{-1}·d^{-1}). In syntrophic ethanol oxidation, EEO and hydrogenotrophic methanogenesis are interdependent: an ethanol oxidizer needs a hydrogenotrophic methanogen that keeps the pH_2 sufficiently low (<14% at standard conditions for $\Delta G_r^{0\prime}$ < 0 kJ·reaction^{-1}) to proceed EEO whereas a hydrogenotrophic methanogen cannot survive without a hydrogen producer.[27] Electrons can be transferred from an ethanol oxidizer to a hydrogenotrophic methanogen via interspecies hydrogen or formate transfer.[28] Ethanol oxidizers and hydrogenotrophic methanogens are not the only potential syntrophic partners because chain elongating microorganisms also oxidize ethanol and produce hydrogen (eq 1). Chain elongating microorganisms, however, can theoretically oxidize ethanol at a much higher pH_2 compared to ethanol oxidizers (as discussed before) which makes the reverse β-oxidation pathway, from a thermodynamic perspective, independent of a hydrogen consuming syntrophic process.

In our microbial community analysis, we observed that all detected OTUs that belonged to the *Desulfovibrionales* order belonged to the sulfate-reducing genus *Desulfovibrio*. *Desulfovibrio vulgaris* can shift its lifestyle from sulfate reducer to ethanol oxidizer in the absence of sulfate.[29] It is therefore likely that *D. vulgaris* (EEO) performed syntrophic ethanol oxidation with the identified hydrogenotrophic methanogen *M. acididurans*. *M acididurans* is an acid-tolerant hydrogenotrophic methanogen that can be active at *p*H 5−7.[30] Presence of acid-tolerant methanogens such as *M. acididurans* explains methanogenic activity in reactors with high concentrations of fatty acids such as sour digesters or, in this case, chain elongation reactors.

Syntrophic ethanol oxidation could be related to the formation of granular sludge, which was observed in the first period of the reactor run.[19] These granules were persistently present in the reactor up to the end of the study at day 240. Syntrophic cocultures of an ethanol oxidizer and a hydrogenotrophic methanogen, have previously been shown to coaggregate,[31] indicating that such syntrophic partnerships may have contributed to granulation in our study. Syntrophic consortia benefit from granulation because intermicrobial distances are short which leads to an efficient interspecies hydrogen transfer.[32] Based on the activity test in our previous study, we calculated that EEO in granular sludge (25.2 ± 1.5% of total ethanol use) was similar compared to suspended sludge (19.3 ± 3.6%). This shows that both sludge types can be used for ethanol upgrading.

4.2. VFA Upgrading: CO_2 Stimulates Heptanoate Production up to 1 L_{CO2}·L^{-1}·d^{-1}. Heptanoate production by VFA upgrading remained constant (~1.8 g·L^{-1}·d^{-1}) at CO_2 loading rates higher than or equal to 1 L_{CO2}·L^{-1}·d^{-1} (Figure 2a). Caproate production by ethanol upgrading, however, was always faster and proportional to the CO_2 loading rate in the tested range (0−2.5 L_{CO2}·L^{-1}·d^{-1}). This observation can be explained by assuming that propionate (electron acceptor for VFA upgrading) and acetate (electron acceptor for ethanol upgrading) compete for the same enzyme system (in chain elongating microorganisms) which could have a higher affinity for acetate. This explanation is supported by our results which show that the rate of ethanol upgrading (butyrate + caproate + caprylate; 131.9 mmol·L^{-1}·d^{-1}) was 44% higher than the rate of VFA upgrading (valerate + heptanoate; 91.7 mmol·L^{-1}·d^{-1}) while acetate and propionate had similar concentrations (~30 mmol·L^{-1}; at 2.5 L_{CO2}·L^{-1}·d^{-1}). The role of electron acceptors on ethanol upgrading and VFA upgrading could be further elucidated by for instance substituting acetate or butyrate with propionate in a similar experiment. Because of the higher apparent affinity for acetate and because acetate is always produced via the reverse β-oxidation pathway, it is a challenge to achieve a high selectivity for odd numbered fatty acids in chain elongation. This study, however, shows that selectivity for odd numbered fatty acids can be increased to some extent by limiting ethanol upgrading: Combined selectivity for valerate and heptanoate at 2.5 L_{CO2}·L^{-1}·d^{-1} was 31% (SI Table S3) and could be increased up to 56% by lowering the CO_2 loading rate to 0.5 L_{CO2}·L^{-1}·d^{-1} (SI Table S5). This shows that the odd−even product ratio in chain elongation can be controlled by limiting syntrophic ethanol oxidation via CO_2 loading rate. So far, continuous odd-numbered fatty acid production by chain elongation was also studied by Grootscholten et al. (2013).[9] Their maximum selectivity for valerate and heptanoate was similar (57%). To what extent selectivity for odd numbered fatty acids can be further increased remains open for future investigation.

4.3. CO_2 is Essential for Both Ethanol Upgrading and VFA Upgrading. Low and decreasing rates of ethanol upgrading and VFA upgrading were observed when CO_2 was not supplied to the reactor (day 211−224). This shows that chain elongation cannot be established as a high rate process without a source of CO_2. Grootscholten et al. (2014) already mentioned that chain elongation without CO_2 may not be possible,[11] although experimental data on complete elimination of (a source of) CO_2 has not been shown to date.

An evident explanation why chain elongation could not be established without CO_2, is that CO_2 is used in anabolic reactions (protein synthesis for growth) by the key chain elongating bacterium *C. kluyveri*. *C. kluyveri* requires both CO_2 and acetate for growth.[18] Growth of *C. kluyveri* was shown to be proportional to the CO_2 uptake and the dissolved CO_2 concentration up to ~3 mmol·L^{-1}.[18] This concentration is

DOI: 10.1021/acs.est.7b04904
Environ. Sci. Technol. 2018, 52, 1496−1505

more than twice as high as compared to the highest observed CO_2 concentration in this study (Table 1), which could imply that growth of such chain elongating microorganisms (and thus chain elongation-activity) may have been limited by CO_2 availability during the entire study. Although presence of *C. kluyveri* could not be confirmed to species level in the bacterial community, it is evident from our results that CO_2 is essential for MCFA production by both ethanol upgrading and VFA upgrading.

At 0 $L_{CO2}{\cdot}L^{-1}{\cdot}d^{-1}$, hydrogenotrophic methanogenic activity was almost entirely suppressed and this resulted in a buildup of hydrogen until 41.6% (Table 1). Although this hydrogen may have reduced the growth rate of chain elongating microorganisms such as *C. kluyveri* (e.g., ref 33), it is unlikely that this caused the total collapse of the process. A coculture of *C. kluyveri* and *Clostridium autoethanogenum* was able to perform chain elongation at an initial pH_2 of ≥100%.[34] Furthermore, earlier work with open cultures demonstrated MCFA production rates up to 28.6 mmol $C{\cdot}L^{-1}{\cdot}d^{-1}$ at an initial pH_2 of 150%.[6] Angenent et al. (2016) recently explained why chain elongation through the reverse β-oxidation pathway still proceeds at high pH_2, albeit at lower rate, by means of a stoichiometric and thermodynamic model.[16] This shows that chain elongation does not collapse at increased hydrogen concentrations. A systematic investigation on the effect of pH_2 on chain elongation, however, remains open for future studies.

When CO_2 was not supplied, we still measured a CO_2 concentration of 0.07% in the headspace (0.03 $mmol{\cdot}L^{-1}$). This was possibly a result of fermentation of yeast extract or decaying biomass which could have contributed to chain elongating activity observed. Another chain elongation study showed that fermentation of yeast extract (1 g; 34 mmol C) results in production of acetate (11 mmol C), butyrate (3 mmol C) and CO_2 (4 mmol C; data not shown).[14] This means that yeast extract could have contributed to 4−7% of total formed products and to CO_2 production with an equivalent of ∼0.1 $L_{CO2}{\cdot}L^{-1}{\cdot}d^{-1}$ in the present study.

At 0 $L_{CO2}{\cdot}L^{-1}{\cdot}d^{-1}$, we could not identify a steady state because rates were decreasing. For example, the valerate production rate was 4.5 $g{\cdot}L^{-1}{\cdot}d^{-1}$ on day 216 and 3.2 $g{\cdot}L^{-1}{\cdot}d^{-1}$ on day 222. To prevent the likelihood of a further collapse of the process, it was decided to supply the reactor with CO_2 again with 1 $L_{CO2}{\cdot}L^{-1}{\cdot}d^{-1}$ on day 224. As a result, chain elongation activity increased and had similar steady state values as before at the same CO_2 loading rate (SI Tables S7 and S4). This does not only confirm that CO_2 is the crucial control parameter, but also that CO_2-dependent activity (i.e., chain elongation and syntrophic ethanol oxidation) is repairable.

5. OUTLOOK: CO_2 CONTROL IN CHAIN ELONGATION WITH RESIDUAL SUBSTRATES

Depending on the anticipated type of chain elongation process, ethanol upgrading is either desired (should be stimulated) or not (should be minimized). Our results show that a high CO_2 loading rate must be selected when ethanol upgrading is desired whereas a low CO_2 loading rate must be selected when ethanol upgrading is undesired.

Ethanol upgrading can be desired when the value of caproate is relatively high compared to ethanol.[12,13] Currently, purified caproic acid (1.00 €·kg^{-1}; 19.36 €·kmol C^{1-}) has a higher value per carbon atom than ethanol (0.52 €·kg^{-1}; 11.98 €·kmol C^{1-}).[35] To produce 1 kg caproic acid (€1), 1.19 kg ethanol is needed (€0.62) so ethanol upgrading is therefore from a feedstock to product point of view economically feasible. Moreover, the potential of using (lignocellulosic) bioethanol as feedstock for the biotechnological conversion into other higher-value biobased platform chemicals has already been considered.[36] Caproate could eventually also be used for production of 1-hexene (via 1-hexanol) for jet and diesel fuels.[37] In this way, car fuel is converted into aviation fuel. Agler et al. (2012) mentioned that ethanol upgrading from undistilled fermentation broth could be useful to circumvent distillation of ethanol which is energetically expensive.[12] When an ethanol upgrading process is desired, the CO_2 loading rate should be high enough to sufficiently stimulate syntrophic ethanol oxidation. When the CO_2 loading rate is too high, however, this could become detrimental because the CO_2 loading rate is inversely related with the pH_2 (Table 1). When the pH_2 becomes too low, anaerobic oxidation of MCFAs is thermodynamically feasible.[22] This was likely the case when Grootscholten et al. (2014) increased the CO_2 loading rate to a chain elongation reactor from 2.4 to 4.8 $L_{CO2}{\cdot}L^{-1}{\cdot}d^{-1}$ which resulted in acetate accumulation instead of chain elongation.[11] To what extent ethanol upgrading can be further increased without oxidation of products remains to be investigated. Possibly, one can control ethanol upgrading by supplying CO_2 while controlling the pH_2 at 0.007%. In theory, this does thermodynamically prevent oxidation of both VFAs and MCFAs under standard conditions ($\Delta Gr' > 0$ $kJ{\cdot}reaction^{-1}$). CO_2 does not necessarily need to be supplied externally because it can also be produced through primary fermentation reactions (e.g., fermentation of sugars). This allows the conversion of a sugar rich feedstock into MCFAs in only one reactor vessel without external CO_2 supply. However, there is an argument to prefer to separate primary fermentation from chain elongation and to supply CO_2 externally because this allows easier control of the pH_2 during chain elongation.[11]

Ethanol upgrading is not desired when (costly and procured) ethanol must be used efficiently. This means that (1) ethanol should primarily be used for VFA upgrading and (2) EEO should be minimized. Ethanol upgrading is also not desired when a higher odd numbered MCFA (e.g., heptanoate) fraction is wanted because ethanol upgrading always results in even-numbered MCFA production. Ethanol upgrading is less efficient than VFA upgrading because ethanol upgrading requires more ethanol to produce MCFAs than VFA upgrading. For example, ethanol upgrading requires three moles of ethanol to produce 1 mol of caproate whereas VFA upgrading requires only 1.2 (starting from butyrate) or 2.4 (starting from acetate) moles of ethanol. Ge et al. (2015) therefore mentioned that ethanol use is reduced when primary fermentation is directed toward butyrate instead of acetate as electron acceptor for chain elongation.[22]

If ethanol upgrading is undesired, CO_2 loading rate should be sufficiently low to limit EEO. When working with residual substrates, however, CO_2 loading rate may be more challenging to control than in this study in which a synthetic medium and gaseous CO_2 with a mass flow controller was used. This is because residual substrates may contain initial dissolved CO_2, or CO_2 is produced in situ from the residues. For example, Ge et al. (2015) fed undistilled fermentation broth from the bioethanol industry to a chain elongation reactor without external CO_2 supply.[22] They still observed a CO_2 concentration of ∼0.4% which could be derived from primary fermentation reactions. Although this CO_2 likely enabled chain elongation activity in their study, its supply was not controlled during the

DOI: 10.1021/acs.est.7b04904
Environ. Sci. Technol. 2018, 52, 1496−1505

process. To avoid in situ CO_2 production in chain elongation, a two-stage conversion (primary fermentation followed by chain elongation) can be considered.[11] Still, effluent from a primary fermentation reactor can contain high concentrations of CO_2 (up to 39% in the headspace; 10 mmol·L^{-1}).[38] This means that, if ethanol upgrading is undesired, the CO_2 concentration in this effluent must be reduced prior to feeding it to the chain elongation stage. This could be performed by supplying hydrogen to the primary fermentation stage to facilitate homoacetogenesis to produce acetate[39] or hydrogenotrophic methanogenesis to produce methane,[40] resulting in consumption of CO_2. As an alternative, the CO_2 concentration could be reduced by stripping with nitrogen or upgrading it with acetate into butyrate using a bioelectrochemical system.[41] Evidently, producing acetate or butyrate is advantageous since it has a higher value than methane. Limiting EEO (by limiting hydrogenotrophic methanogenesis) could also be performed in a different way than adjusting the CO_2 loading rate. For example, Agler et al. (2014) demonstrated that activity of hydrogenotrophic methanogens decreased with increasing concentrations of undissociated butyric acid.[13] This indicates that EEO may also be limited by toxicity of fatty acids under conditions with residual substrates.

■ ASSOCIATED CONTENT

Supporting Information

The Supporting Information is available free of charge on the ACS Publications website at DOI: 10.1021/acs.est.7b04904.

An overview of dominant and considered processes in this study (Table S1), materials and methods for microbial community analysis, calculations on carbon fluxes (Table S2), a graphical summary of reactor performance with rate in mmol C·L^{-1}·d^{-1} (Figure S1), steady state concentrations/rates/carbon selectivities (Table S3−S7), results of thermodynamic analysis (Figure S2), results of bacterial community analysis (Figure S3) and results of archaeal community analysis (Table S8) (PDF)

■ AUTHOR INFORMATION

Corresponding Author

*Phone: +31 317 483 447; e-mail: david.strik@wur.nl.

ORCID

Mark Roghair: 0000-0002-0256-215X

Present Address

#(T.H.) Biobased Chemistry & Technology, Wageningen University & Research, Bornse Weilanden 9, 6708 WG, Wageningen, The Netherlands.

Notes

The authors declare no competing financial interest.

■ ACKNOWLEDGMENTS

This work has been carried out with a grant from the BE-BASIC program FS 01.006 (www.be-basic.org). Research of P.H.A.T. is supported by the Soehngen Institute of Anaerobic Microbiology (SIAM) Gravitation grant (024.002.002) of the Netherlands Ministry of Education, Culture and Science and the Netherlands Organisation for Scientific Research (NWO).We thank the peer reviewers for their valuable comments and suggestions.

■ ABBREVIATIONS

VFAs	volatile fatty acids
MCFAs	medium chain fatty acids
EEO	excessive ethanol oxidation
HRT	hydraulic retention time

■ REFERENCES

(1) Agler, M. T.; Wrenn, B. A.; Zinder, S. H.; Angenent, L. T. Waste to bioproduct conversion with undefined mixed cultures: the carboxylate platform. *Trends Biotechnol.* **2011**, *29* (2), 70−78.

(2) Anneken, D. J.; Both, S.; Christoph, R.; Fieg, G.; Steinberner, U.; Westfechtel, A., Fatty Acids. In *Ullmann's Encyclopedia of Industrial Chemistry*; Wiley-VCH Verlag GmbH & Co. KGaA: 2000.

(3) Gervajio, G. C. Fatty Acids and Derivatives from Coconut Oil. In *Bailey's Industrial Oil and Fat Products*; John Wiley & Sons, Inc., 2005.

(4) G Cassman, K.; Liska, A. J. Food and fuel for all: realistic or foolish? *Biofuels, Bioprod. Biorefin.* **2007**, *1* (1), 18−23.

(5) Sheil, D.; Casson, A.; Meijaard, E.; Van Noordwjik, M.; Gaskell, J.; Sunderland-Groves, J.; Wertz, K.; Kanninen, M. *The Impacts and Opportunities of Oil Palm in Southeast Asia: What Do We Know and What Do We Need to Know?*; Center for International Forestry Research (CIFOR): Bogor, Indonesia, 2009.

(6) Steinbusch, K. J. J.; Hamelers, H. V. M; Plugge, C. M.; Buisman, C. J. N. Biological formation of caproate and caprylate from acetate: fuel and chemical production from low grade biomass. *Energy Environ. Sci.* **2011**, *4* (1), 216−224.

(7) Grootscholten, T. I. M.; Steinbusch, K. J. J.; Hamelers, H. V. M; Buisman, C. J. N. Chain elongation of acetate and ethanol in an upflow anaerobic filter for high rate MCFA production. *Bioresour. Technol.* **2012**, *135*, 440−445.

(8) Grootscholten, T. I. M.; Steinbusch, K. J. J.; Hamelers, H. V. M; Buisman, C. J. N. Improving medium chain fatty acid productivity using chain elongation by reducing the hydraulic retention time in an upflow anaerobic filter. *Bioresour. Technol.* **2013**, *136*, 735−738.

(9) Grootscholten, T. I. M.; Steinbusch, K. J. J.; Hamelers, H. V. M; Buisman, C. J. N. High rate heptanoate production from propionate and ethanol using chain elongation. *Bioresour. Technol.* **2013**, *136* (0), 715−718.

(10) Grootscholten, T. I. M.; dal Borgo, F. K.; Hamelers, H. V. M.; Buisman, C. J. N. Promoting chain elongation in mixed culture acidification reactors by addition of ethanol. *Biomass Bioenergy* **2013**, *48*, 10−16.

(11) Grootscholten, T. I. M.; Strik, D. P. B. T. B.; Steinbusch, K. J. J.; Buisman, C. J. N.; Hamelers, H. V. M Two-stage medium chain fatty acid (MCFA) production from municipal solid waste and ethanol. *Appl. Energy* **2014**, *116*, 223−229.

(12) Agler, M. T.; Spirito, C. M.; Usack, J. G.; Werner, J. J.; Angenent, L. T. Chain elongation with reactor microbiomes: Upgrading dilute ethanol to medium-chain carboxylates. *Energy Environ. Sci.* **2012**, *5* (8), 8189−8192.

(13) Agler, M. T.; Spirito, C. M.; Usack, J. G.; Werner, J. J.; Angenent, L. T. Development of a highly specific and productive process for n-caproic acid production: applying lessons from methanogenic microbiomes. *Water Sci. Technol.* **2014**, *69* (1), 62−68.

(14) Chen, W. S.; Ye, Y.; Steinbusch, K. J. J.; Strik, D. P. B. T. B.; Buisman, C. J. N. Methanol as an alternative electron donor in chain elongation for butyrate and caproate formation. *Biomass Bioenergy* **2016**, *93*, 201−208.

(15) Kucek, L. A.; Nguyen, M.; Angenent, L. T. Conversion of l-lactate into n-caproate by a continuously fed reactor microbiome. *Water Res.* **2016**, *93*, 163−171.

(16) Angenent, L. T.; Richter, H.; Buckel, W.; Spirito, C. M.; Steinbusch, K. J. J.; Plugge, C. M.; Strik, D. P. B. T. B.; Grootscholten, T. I. M.; Buisman, C. J. N.; Hamelers, H. V. M Chain Elongation with Reactor Microbiomes: Open-Culture Biotechnology To Produce Biochemicals. *Environ. Sci. Technol.* **2016**, *50* (6), 2796−2810.

(17) Coma, M.; Vilchez-Vargas, R.; Roume, H.; Jauregui, R.; Pieper, D. H.; Rabaey, K. Product Diversity Linked to Substrate Usage in

DOI: 10.1021/acs.est.7b04904
Environ. Sci. Technol. 2018, 52, 1496−1505

Chain Elongation by Mixed-Culture Fermentation. *Environ. Sci. Technol.* **2016**, *50* (12), 6467−6476.
(18) Tomlinson, N.; Barker, H. A. Carbon dioxide and acetate utilization by clostridium kluyveri. I. Influence of nutritional conditions on utilization patterns. *J. Biol. Chem.* **1954**, *209*, 585−595.
(19) Roghair, M.; Strik, D. P. B. T. B.; Steinbusch, K. J. J.; Weusthuis, R. A.; Bruins, M. E.; Buisman, C. J. N. Granular sludge formation and characterization in a chain elongation process. *Process Biochem.* **2016**, *51* (10), 1594−1598.
(20) Steinbusch, K. J. J.; Hamelers, H. V. M; Buisman, C. J. N. Alcohol production through volatile fatty acids reduction with hydrogen as electron donor by mixed cultures. *Water Res.* **2008**, *42* (15), 4059−4066.
(21) Kleerebezem, R.; Van Loosdrecht, M. C. M. A generalized method for thermodynamic state analysis of environmental systems. *Crit. Rev. Environ. Sci. Technol.* **2010**, *40* (1), 1−54.
(22) Ge, S.; Usack, J. G.; Spirito, C. M.; Angenent, L. T. Long-term n-caproic acid production from yeast-fermentation beer in an anaerobic bioreactor with continuous product extraction. *Environ. Sci. Technol.* **2015**, *49* (13), 8012−8021.
(23) Lonkar, S.; Fu, Z.; Holtzapple, M. Optimum alcohol concentration for chain elongation in mixed-culture fermentation of cellulosic substrate. *Biotechnol. Bioeng.* **2016**, *113* (12), 2597−2604.
(24) Sander, R. *Compilation of Henry's Law Constants for Inorganic and Organic Species of Potential Importance in Environmental Chemistry*; Max-Planck Institute of Chemistry, Air Chemistry Department Mainz: Germany, 1999.
(25) Seedorf, H.; Fricke, W. F.; Veith, B.; Bruggemann, H.; Liesegang, H.; Strittmatter, A.; Miethke, M.; Buckel, W.; Hinderberger, J.; Li, F.; Hagemeier, C.; Thauer, R. K.; Gottschalk, G. The genome of Clostridium kluyveri, a strict anaerobe with unique metabolic features. *Proc. Natl. Acad. Sci. U. S. A.* **2008**, *105* (6), 2128−2133.
(26) Schmidt, J. E.; Ahring, B. K. Effects of hydrogen and formate on the degradation of propionate and butyrate in thermophilic granules from an upflow anaerobic sludge blanket reactor. *Appl. Environ. Microbiol.* **1993**, *59* (8), 2546−2551.
(27) Schink, B. Energetics of syntrophic cooperation in methanogenic degradation. *Microbiol. Mol. Biol. Rev.* **1997**, *61* (2), 262−280.
(28) Stams, A. J. M.; Plugge, C. M. Electron transfer in syntrophic communities of anaerobic bacteria and archaea. *Nat. Rev. Microbiol.* **2009**, *7* (8), 568−577.
(29) Plugge, C. M.; Zhang, W.; Scholten, J. C. M.; Stams, A. J. M. Metabolic flexibility of sulfate-reducing bacteria. *Front. Microbiol.* **2011**, *2* (May), 81.
(30) Savant, D. V.; Shouche, Y. S.; Prakash, S.; Ranade, D. R. Methanobrevibacter acididurans sp. nov., a novel methanogen from a sour anaerobic digester. *Int. J. Syst. Evol. Microbiol.* **2002**, *52* (4), 1081−1087.
(31) Ishii, S.; Kosaka, T.; Hori, K.; Hotta, Y.; Watanabe, K. Coaggregation facilitates interspecies hydrogen transfer between Pelotomaculum thermopropionicum and Methanothermobacter thermautotrophicus. *Appl. Environ. Microbiol.* **2005**, *71* (12), 7838−7845.
(32) Kouzuma, A.; Kato, S.; Watanabe, K. Microbial interspecies interactions: recent findings in syntrophic consortia. *Front. Microbiol.* **2015**, *6*, 477.
(33) Schoberth, S.; Gottschalk, G. Considerations on the energy metabolism of Clostridium kluyveri. *Arch. Microbiol.* **1969**, *65* (4), 318−328.
(34) Diender, M.; Stams, A. J. M.; Sousa, D. Z. Production of medium-chain fatty acids and higher alcohols by a synthetic co-culture grown on carbon monoxide or syngas. *Biotechnol. Biofuels* **2016**, *9* (1), 82.
(35) Kleerebezem, R.; Joosse, B.; Rozendal, R.; Van Loosdrecht, M. C. M. Anaerobic digestion without biogas? *Rev. Environ. Sci. Bio/Technol.* **2015**, *14* (4), 787−801.
(36) Weusthuis, R. A.; Aarts, J. M. M. J. G.; Sanders, J. P. M. From biofuel to bioproduct: is bioethanol a suitable fermentation feedstock for synthesis of bulk chemicals? *Biofuels, Bioprod. Biorefin.* **2011**, *5* (5), 486−494.
(37) Harvey, B. G.; Meylemans, H. A. 1-Hexene: A renewable C6 platform for full-performance jet and diesel fuels. *Green Chem.* **2014**, *16* (2), 770−776.
(38) Min, K.; Khan, A.; Kwon, M.; Jung, Y.; Yun, Z.; Kiso, Y. Acidogenic fermentation of blended food-waste in combination with primary sludge for the production of volatile fatty acids. *J. Chem. Technol. Biotechnol.* **2005**, *80* (8), 909−915.
(39) Ni, B. J.; Liu, H.; Nie, Y. Q.; Zeng, R. J.; Du, G. C.; Chen, J.; Yu, H. Q. Coupling glucose fermentation and homoacetogenesis for elevated acetate production: Experimental and mathematical approaches. *Biotechnol. Bioeng.* **2011**, *108* (2), 345−353.
(40) Luo, G.; Johansson, S.; Boe, K.; Xie, L.; Zhou, Q.; Angelidaki, I. Simultaneous hydrogen utilization and in situ biogas upgrading in an anaerobic reactor. *Biotechnol. Bioeng.* **2012**, *109* (4), 1088−1094.
(41) Raes, S. M. T.; Jourdin, L.; Buisman, C. J. N.; Strik, D. P. B. T. B. Continuous Long-Term Bioelectrochemical Chain Elongation to Butyrate. *ChemElectroChem* **2017**, *4* (2), 386−395.

DOI: 10.1021/acs.est.7b04904
Environ. Sci. Technol. 2018, 52, 1496−1505